ACS Catalysis

Research Article

pubs.acs.org/acscatalysis

Mechanistic Study of Glucose-to-Fructose Isomerization in Water Catalyzed by $[Al(OH)_2(aq)]^+$

Jinqiang Tang, Xiawei Guo, Liangfang Zhu,* and Changwei Hu*

Key Laboratory of Green Chemistry and Technology, Ministry of Education, College of Chemistry, Sichuan University, Chengdu, Sichuan 610064, P. R. China

Supporting Information

ABSTRACT: The nature of the active aluminum species and their interaction with glucose in water are studied to establish a detailed mechanism for understanding $AlCl_3$-catalyzed glucose-to-fructose isomerization. The combination of activity results with electrospray ionization tandem mass spectrometry (ESI-MS/MS) reveal that $[Al(OH)_2(aq)]^+$ species contribute a lot to the isomerization. Attenuated total reflection infrared spectroscopy (ATR-IR) results show that glucose undergoes a ring-opening process which is accelerated by the $[Al(OH)_2(aq)]^+$ species. The binding of acyclic glucose with $[Al(OH)_2(aq)]^+$ species occurs at the C1−O and C2−O positions of glucose, which initiates the hydride shift of the aldose-to-ketose isomerization. The in situ ^{27}Al NMR data elucidate the maintenance of the hexa-coordinated form of Al species throughout the reaction. An obvious kinetic isotope effect occurs with the C2 deuterium-labeled glucose, confirming that the intramolecular hydride shift from the C2 to C1 positions of glucose is the rate-limiting step for the isomerization. The apparent activation energy (E_a) of the $AlCl_3$-catalyzed glucose-to-fructose isomerization reaction is estimated to be 110 ± 2 kJ·mol^{-1}.

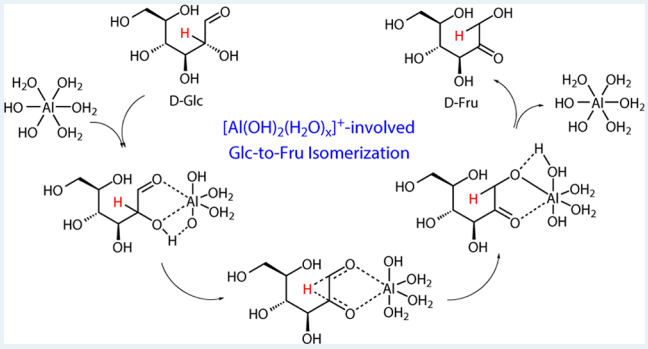

KEYWORDS: *glucose, isomerization, fructose, mechanism, $AlCl_3$ catalyst*

INTRODUCTION

Glucose-to-fructose isomerization is not only an important reaction for the production of high-fructose corn syrups but is also a significant intermediate step in the production of 5-hydroxymethylfurfural (HMF) from glucose.[1−4] Several types of Lewis acid or Brønsted base catalysts, e.g., Sn-Beta,[5−10] H-USY zeolites,[11] hybrid solid bases of MCM molecular sieves,[12] functionalized MOFs,[13] zirconium carbonate,[14] Mg−Al hydrotalcites,[15,16] metal chlorides,[17−27] and organic amines[28,29] were used to catalyze glucose-to-fructose isomerization.

Glucose-to-fructose isomerization in aqueous media generally involves three steps (Scheme 1): (1) aldose ring-opening, (2) aldose-to-ketose isomerization in chain forms, and (3) ketose ring-closure.[18,30] In catalyst-free aqueous solutions, the ring-opening first proceeded from the protonation of O5 with water as the proton source,[31,32] but the activity for this isomerization reaction was poor. In the presence of Lewis acids, it was well accepted that the catalytically active metal species formed in aqueous solution induced the ring-opening of glucose followed by an intramolecular hydride shift step.[10,18,33] Mushrif and co-workers[19] used molecular dynamics to study the mechanism of $CrCl_3$-catalyzed glucose-to-fructose isomerization. In the presence of $CrCl_3$, they found that $[Cr(OH)(H_2O)_5]^{2+}$ was active for the ring-opening of glucose by deprotonation of O1−H on glucose and loss of the proton to the OH group on the partially hydrolyzed Cr(III) center. While for Sn-Beta, Davis and co-workers[10] used B3LYP(2) and MP2 levels of theory to investigate the isomerization mechanism. It was suggested that the actual active site of Sn-Beta was the $(SiO)_3Sn(OH)$ species, with which the ring-opening proceeded through the metallization of O5 on glucose with Sn and then the deprotonation of the O1−H on glucose to the OH group of $Sn-(OSiH_3)_3-OH$. In these catalytic systems, water helps the generation of active Lewis acid species.[5,19]

As a cheap and low-toxic catalyst, $AlCl_3$ behaved well in the glucose-to-fructose isomerization in aqueous media.[17,18,22−26] However, the active species, normally existed as hydrolyzed forms, and their interaction with glucose under the reaction conditions are still lack of detailed information. The distribution of hydrolyzed $AlCl_3$ species in aqueous media depends on many parameters, e. g., pH value, concentration of $AlCl_3$, temperature, and so on. It is generally accepted that Al^{3+} exists in the form of (1) hexa-coordinated $[Al(aq)]^{3+}$ in strong acid solutions (pH < 3.0), (2) hexa-coordinated monomers ($[Al(OH)(aq)]^{2+}$, $[Al(OH)_2(aq)]^+$), dimers ($[Al_2(OH)_2(aq)]^{4+}$), trimers ($[Al_3(OH)_4(aq)]^{5+}$), etc., at pH values of 3.0−7.0, and (3) tetra-coordinated $[Al(OH)_4]^-$ accompanied by some polymers (Al_{13}-mer, Al_{30}-mer) in basic

Received: February 16, 2015
Revised: July 22, 2015
Published: July 22, 2015

DOI: 10.1021/acscatal.5b01237
ACS Catal. 2015, 5, 5097−5103

Scheme 1. Generally Accepted Pathway for the Isomerization of Glucose-to-Fructose

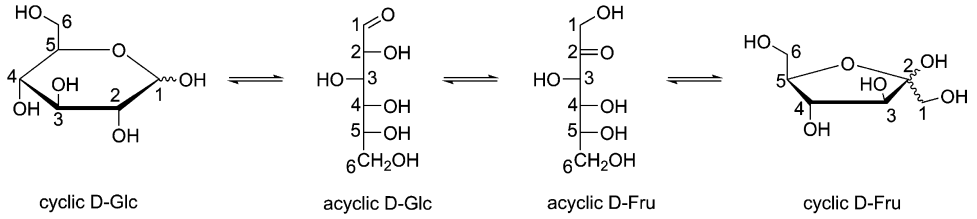

solutions (pH > 7.0) at room temperature.[34] Casey's group[35] proposed a five-coordinated $[Al(OH)(H_2O)_4]^{2+}$ ion as the predominant form of $[Al(OH)\ (aq)]^{2+}$ under ambient conditions at pH 4.3−7.0 using Car−Parrinello molecular dynamics (CPMD) simulations. While $[Al(OH)_2(H_2O)_4]^{+}$ was thought to be the dominant species in dilute $AlCl_3$(aq) (0.02−100 mM) solution from the results of ESI-Q-MS experiments.[36,37] In high temperature aqueous solution, abundant polymers including Al_{13}-mer and Al_{30}-mer also existed due to severe hydrolysis.[38] In the glucose-containing aqueous media, the possible interaction between aluminum species with glucose makes the situation more complicated. Some researchers thought that $[Al(OH)(H_2O)_5]^{2+}$ might be the active species in the catalytic conversion of glucose in water, analogous to $[Cr(OH)(H_2O)_5]^{2+}$ in the case of $CrCl_3$.[17,18,22] In our previous work,[39] it was found that the $[Al(OH)\ (aq)]^{2+}$ and $[Al(OH)_2(aq)]^{+}$ species were both thermodynamically stable in water. However, the detailed mechanistic behavior of the aluminum species under actual experimental conditions are still lack. In the present work, the nature of the active species from $AlCl_3$ and their interaction with glucose in water are studied to establish a more detailed mechanism for understanding the glucose-to-fructose isomerization by attenuated total reflection infrared spectroscopy (ATR-IR), electrospray ionization tandem mass spectrometry (ESI-MS/MS), $^{1}H/^{13}C/^{27}Al$ NMR, and kinetic isotope effect (KIE) methods.

EXPERIMENTAL SECTION

Materials. C2 deuterium-labeled glucose (C2 D-labeled glucose, 98%) was obtained from Cambridge Isotope Laboratories (CIL), Inc. Sn-Beta was purchased from Science Techno, Inc. (Dalian, Liaoning, China). The ultrapure water of 18.25 MΩ·cm^{-1} (298 K) was used after degasification. All other chemicals were purchased from Alfa Aesar and used as received.

Catalytic Reaction. In a typical experiment, an aqueous solution of reacting amount of glucose and $AlCl_3{\cdot}6H_2O$ was added into the reactor (pressure vessel, heavy wall, 15 mL, Synthware Glass, Beijing). The whole reaction was carried out under autogenous pressures with stirring. The reactor tube was removed from the oil-bath after the reaction time reached and, then, quenched with cold water. The liquid products were analyzed by HPLC (DIONEX U3000, Thermo Fisher Scientific), equipped with a Refractive Index detector (RI-101, Shodex) and an aminex column (HPX-87H, 300 mm × 7.8 mm, Bio-Rad). The eluent was dilute H_2SO_4 (5 mM) flowing at a rate of 0.60 mL·min^{-1} with the column temperature maintained at 323 K. The concentrations of all components were determined by comparison to standard calibration curves. The conversion of glucose (X), yield (Y), and selectivity (S) to products, as well as the carbon balance are defined as follows:

$$X = (\text{moles of glucose reacted}/\text{moles of starting glucose}) \times 100\%$$

$$Y = (\text{moles of products obtained}/\text{moles of starting glucose}) \times 100\%$$

$$S = (\text{moles of products obtained}/\text{moles of glucose reacted}) \times 100\%$$

$$\text{carbon balance} = (\text{output of carbon}/\text{input of carbon}) \times 100\%$$

Kinetics Study. The kinetics study on the conversion of glucose were investigated by varying the concentration of $AlCl_3$, reaction temperature, and time. The reaction rate constant (k) was calculated by plotting ln[Glc] versus t at low conversion of glucose. Initial turnover frequency (TOF) was calculated at the start of the reaction from a kinetic profiles. The apparent activation energy (E_a) was estimated by plotting ln k versus $1/T$ through the Arrhenius equation.

ESI-MS/MS. ESI-MS were collected in continuum mode. A Micromass Quattro Micro mass spectrometer (Waters) was used with the following operating parameters: capillary voltage, 2.8 kV; extractor voltage, 5 V; sample cone voltage, 20 V; source temperature, 363 K; desolvation temperature, 423 K; cone gas (N_2) flow, 40 L·h^{-1}. A collision energy of 20 eV was used for the collision-induced dissociation stage in the MS/MS measurements. The data acquisition and analyses were performed using Masslynx v 4.1 software (Waters).

ATR-IR Spectrometry. The ReactIR iC10 system (Mettler Toledo) equipped with a liquid nitrogen cooled mercury cadmium telluride (MCT) detector was used for the acquisition of mid-IR spectra with time. Measurements were taken optically using a DiComp immersion probe and ZnSe as an ATR crystal. The instrument was computer-controlled using software iC IR Version 4.1.882 (Mettler Toledo) for data acquisition. During the entire process, high purity nitrogen at a flow rate of 2.5 L·min^{-1} was supplied continuously to ensure the light path clean, and each spectrum represented 256 coadded scans measured every minute at a resolution of 8 cm^{-1} in the range of 1950−650 cm^{-1} with the Happ-Genzel apodization method. Reaction profiles were generated from those data by taking peak heights and given as absorbance units relative to zero.

NMR Spectrometry. NMR spectra were obtained using an Advance II 400 MHz NMR spectrometer (Bruker). ^{1}H NMR spectra were measured at 400.13 MHz (pulse width, 9.75 μs; acquisition time, 4.0894 μs; 16 scans; 298 ± 1 K; D_2O for field lock; TSP in capillary as external standard for ^{1}H δ 0.00). ^{13}C NMR spectra were measured at 100.62 MHz (pulse width, 9.80 μs; acquisition time, 1.3631 μs; 256 scans; 298 ± 1 K; D_2O for field lock; TSP in capillary as external standard for ^{13}C δ 0.00). In-situ ^{27}Al NMR spectra were measured at 104.27 MHz (pulse width, 17.42 μs; acquisition time, 0.7864 s; 128 scans; 383 ± 1 K; D_2O for field lock), where a thick-wall NMR tube (S-5-500-HW-7, NORELL) containing 0.8 mL of the reaction mixtures (1.0 mL D_2O, 0.25 M Glc, 25.0 mM $AlCl_3$,) was heated to 383 K. The ^{27}Al NMR spectra were recorded every 6 min for 2.0 h.

DOI: 10.1021/acscatal.5b01237
ACS Catal. 2015, 5, 5097−5103

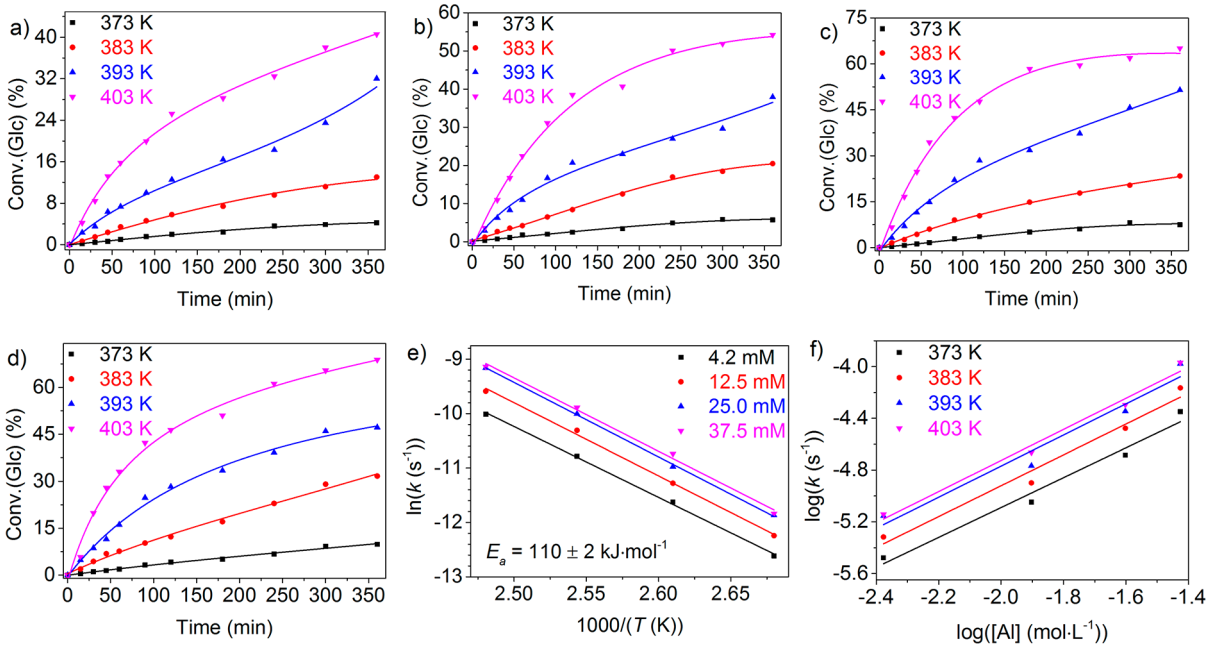

Figure 1. Glucose-to-fructose isomerization with time in water catalyzed with (a) 4.2, (b) 12.5, (c) 25.0, and (d) 37.5 mM of $AlCl_3$. (e) Plots of ln k vs $1/T$. (f) Plots of log k vs log[Al]. Reaction conditions: 1.0 mL H_2O, 0.25 M Glc.

RESULTS AND DISCUSSION

Kinetics Study. The $AlCl_3$-catalyzed glucose conversion in water produced fructose as the main product under the reaction conditions investigated. Small amounts of HMF, formic acid (FA), and levulinic acid (LA) were also detected, which might be derived from the dehydration of fructose to HMF and the further rehydration of HMF.[22,23] The kinetics studies were performed by varying the concentration of $AlCl_3$, reaction temperature, and time. The results are shown in Figure 1a–d. Based on the kinetics data, the k value and initial TOF of the $AlCl_3$-catalyzed conversion of glucose were obtained (Table S1).[40] The k value increased with the increase of temperature and the concentration of $AlCl_3$, and the initial TOF increased with increasing the temperature but decreased with increasing the concentration of $AlCl_3$. The E_a of the $AlCl_3$-catalyzed glucose-to-fructose isomerization was estimated to be 110 ± 2 kJ·mol^{-1} (Figure 1e), which was higher than that of $CrCl_3$ catalyst (59–64 kJ·mol^{-1})[17,20] and compatible to that of Sn-Beta (85–108 kJ·mol^{-1})[7,9,10] or some typical base catalysts such as NaOH and hydrotalcite (121–129 kJ·mol^{-1}).[41−43]

The activity of $AlCl_3$ was also compared with that of $CrCl_3$, $SnCl_4$, and Sn-Beta under the same reaction conditions. The results are shown in Table 1 and Figure S1.[40] Although higher k and initial TOF were obtained over $CrCl_3$ and Sn-Beta catalysts, $AlCl_3$ exhibited higher selectivity to fructose and better carbon balance than other catalysts. That is, $AlCl_3$ was an effective catalyst for the isomerization of glucose to fructose.

Determination of the Active Species. In our previous computational work,[39] it was found that $[Al(OH)(aq)]^{2+}$ and $[Al(OH)_2(aq)]^+$ species were both thermodynamically stable in water. In order to discover the catalytically active species and their interaction with glucose under the actual reaction conditions, ESI-MS/MS methods were used. As shown in Figure S2,[40] the ESI-MS spectrum of aqueous $AlCl_3$ solution in the absence of glucose produced several peaks assigning to the hydrolyzed aluminum species containing $[Al(OH)_2(aq)]^+$ (m/z = 97, 133). However, when the mixtures of $AlCl_3$ and glucose were measured by ESI-MS, much lesser peaks were observed (Figure 2a). Two strong peaks at m/z = 565, 385 appeared, which were assigned to the $[Al(OH)_2(Glc)_3]^+$ and $[Al(OH)_2(Glc)_2]^+$ species, respectively. When MS/MS was performed on the selected peak at m/z = 385 (Figure 2b), the peaks of $[Al(OH)_2(Glc)]^+$ fragments at m/z = 223, 241, 259, 277 and $[Al(OH)_2(aq)]^+$ fragments at m/z = 115, 133 were observed. These results revealed that glucose combined mainly with $[Al(OH)_2(aq)]^+$ species in the $AlCl_3$-containing aqueous glucose solution. When MS/MS was performed on the selected peak at m/z = 565 (Figure S3),[40] the appearance of $[Al(OH)_2(Glc)]^+$ fragments at m/z = 223, 241, 259, 277 also proved the combination of glucose with $[Al(OH)_2(aq)]^+$ species. As a contrast, the ESI-MS/MS spectra of aqueous glucose solution in the absence of $AlCl_3$ only gave out peaks referring to the $[Na+Glc]^+$ species and some unknown fragments (Figure S4).[40]

The ESI-MS/MS spectra of aqueous glucose solution containing different concentrations of $AlCl_3$ (4.2–37.5 mM) were also studied. The results are shown in Figure S5.[40] In all cases, the peaks assigned to $[Al(OH)_2(aq)]^+$ and [Al-

Table 1. Activity Comparisons on Different Catalysts for Glucose-to-Fructose Isomerization[a]

entry	catalysts	X (%)	Y_{Fru} (%)	S_{Fru} (%)	carbon balance (%)	k (10^{-5} s^{-1})	TOF (mol_{Glc}·mol_{Cat}^{-1}·h^{-1})
1	$AlCl_3$·$6H_2O$	31.8	26.3	82.7	100.0	4.5	1.6
2	$CrCl_3$·$6H_2O$	52.3	25.4	48.6	96.0	15.8	5.7
3	$SnCl_4$·$5H_2O$	18.2	4.7	26.0	95.8	2.5	0.9
4	Sn-Beta[b]	67.5	45.3	67.1	91.0	15.8	113.4

[a]Reaction conditions: 1.0 mL H_2O, 0.25 M Glc, 25.0 mM catalyst, 393 K, 180 min. [b]Glc: Sn = 200:1 (mol:mol).

DOI: 10.1021/acscatal.5b01237
ACS Catal. 2015, 5, 5097−5103

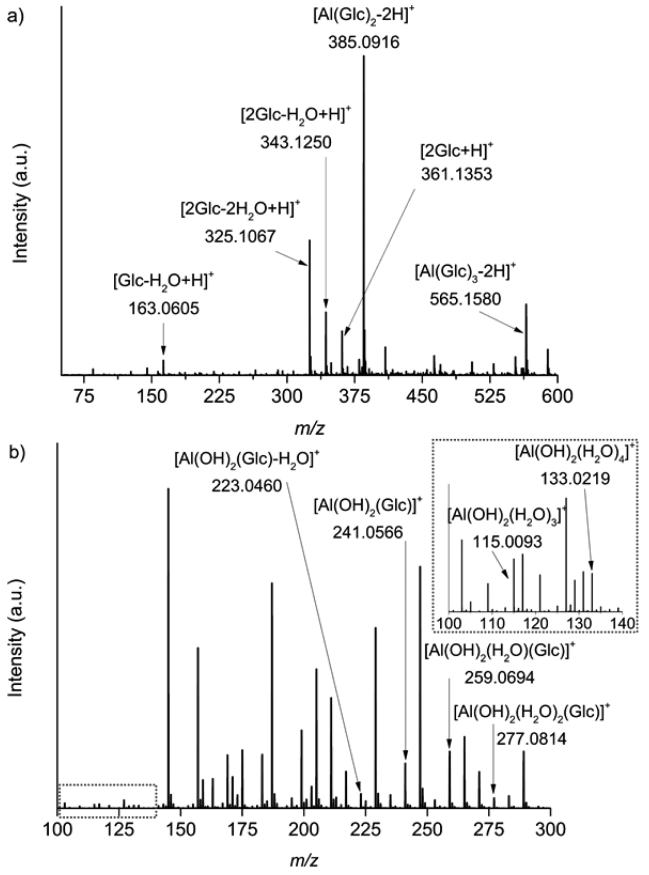

Figure 2. Positive ion mode of (a) ESI-MS and (b) ESI-MS/MS spectra of the $AlCl_3$-containing aqueous glucose solution. (b) MS/MS spectra of the selected $[Al(OH)_2(Glc)_2]^+$ species with m/z of 385. (b inset) Magnified view of the bracketed region. Reaction conditions: 1.0 mL H_2O, 0.25 M Glc, 25.0 mM $AlCl_3$.

$(OH)_2(Glc)\ (aq)]^+$ species were observed, illustrating the presence of the $[Al(OH)_2(aq)]^+$ species and their combination with glucose over the concentration range of $AlCl_3$ investigated.

In order to confirm whether $[Al(OH)_2(aq)]^+$ species was responsible for the isomerization, HCl was added to suppress the hydrolysis of Al^{3+}, which will decrease the concentration of $[Al(OH)_2(aq)]^+$ species in the reaction mixtures. The influence of $AlCl_3$, HCl, and the combination of the two on k and initial TOF of glucose conversion are shown in Table S2.[40] When equimolar amount of HCl and $AlCl_3$ mixtures were used as the catalyst, where the concentration of $[Al(OH)_2(aq)]^+$ species was lower than that with no HCl added, smaller k and initial TOF were obtained. What's more, when excess HCl up to 100 mM was added in the system, where almost only unhydrolyzed Al^{3+} species existed, only 6.9% glucose conversion and 1.4% fructose yield were obtained (Figure S6).[40] Additionally, the activity of $Al(OH)_3$ was also tested, and 7.8% glucose conversion and 6.5% fructose yield were obtained (0.025 mmol $Al(OH)_3$, 180 min, 393 K). When HCl was used solely as the catalyst, the k and initial TOF were extremely low, strongly indicating that the activity was originated from aluminum species. In this situation, because of the complex forms of aluminum species coexisted in the reaction system, we could not exclude the role of unhydrolyzed Al^{3+}, $[Al(OH)(aq)]^{2+}$, and $Al(OH)_3$ species in the reaction. However, in the ESI-MS spectrum, only peaks assigned to $[Al(OH)_2(Glc)]^+$ species were observed, no peaks assigned to $[Al(Glc)]^{3+}$, $[Al(OH)\ (Glc)]^{2+}$, or $[Al(OH)_3(Glc)+nH]^{n+}$ species were observed. These results combined with activity variation with varying pH indicated that the $[Al(OH)_2(aq)]^+$ species contributed a lot to the isomerization reaction. Moreover, the k was found to be increased with increasing the concentration of $AlCl_3$ (Figure 1e), possibly due to the increase of the concentration of the $[Al(OH)_2(aq)]^+$ species in the reaction solutions. The results from linear fit of log k versus log[Al] shown in Figure 1f revealed that the $AlCl_3$-catalyzed glucose-to-fructose isomerization was a first-order reaction with respect to aluminum species. Therefore, the catalytic active species involved in the rate-limiting step should be a mononuclear aluminum species. Combined these results with those of ESI-MS/MS, we estimated that the main active species in glucose-to-fructose isomerization reaction was most possibly the hydrolyzed aluminum species $[Al(OH)_2(aq)]^+$.

Coordination of Aluminum Species. In order to study the coordination of aluminum species in the process of glucose conversion catalyzed by $AlCl_3$, in situ ^{27}Al NMR experiments were performed throughout the reaction process. As shown in Figure 3, a high and sharp resonance peak centered at δ = 1.4

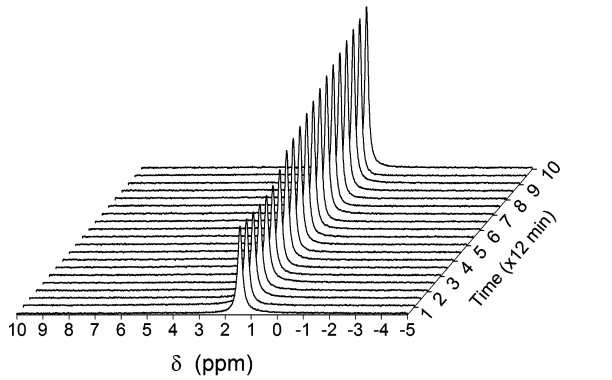

Figure 3. In-situ ^{27}Al NMR spectra of the reaction mixtures with time. Reaction conditions: 0.8 mL of the reaction mixtures (1.0 mL D_2O, 0.25 M Glc, 25.0 mM $AlCl_3$), 383 K.

ppm indicated the presence of hexa-coordinated form of Al center.[38,44] No other resonance peak was observed, except a broad high-frequency resonance peak centered at δ = 77 ppm (Figure S7).[40] The broad peak was deemed to be the background NMR signal derived from the use of Al materials.[45,46] The background resonance was further identified by the Al-free sample (Figure S8).[40] The existence of the peak at δ = 1.4 ppm in the reaction process revealed the maintenance of the hexa-coordinated form of aluminum species throughout the isomerization reaction.

Ring Opening of Glucose. In order to discuss the possible interaction between $[Al(OH)_2(aq)]^+$ species with hydroxyl group in glucopyranose or carbonyl group in acyclic glucose that contributes to the aldose-to-ketose isomerization, ATR-IR spectra of the reaction mixtures was performed at room temperature with time to study the possible ring-opening process of glucose. The results are shown in Figure 4. When glucose was added into water, two peaks at 1055 and 1156 cm^{-1} assigned to the characteristic vibrations of α-D-Glc and deforming of pyranoid ring, respectively,[47−49] were observed, indicating that glucose existed mainly in the form of pyranoid ring in solution, which was consistent with the literature.[50] With time progressed, the intensity of the band at 1055 cm^{-1}

DOI: 10.1021/acscatal.5b01237
ACS Catal. 2015, 5, 5097−5103

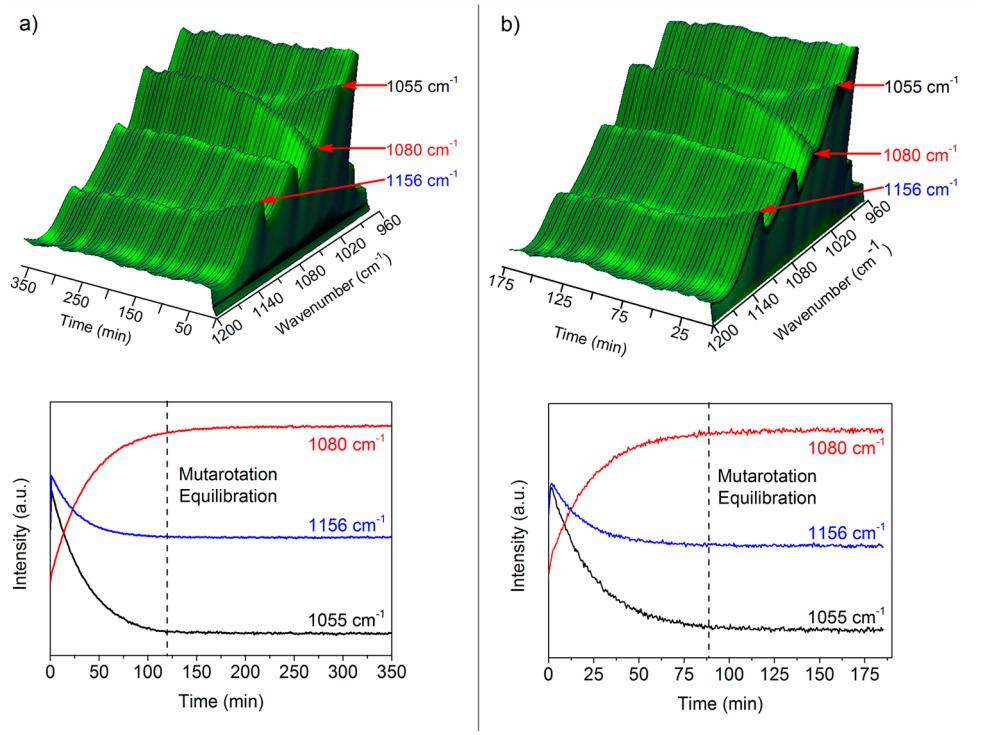

Figure 4. ATR-IR spectra of aqueous glucose solution with time at room temperature (a) in the absence or (b) presence of $AlCl_3$. Reaction conditions: 10 mL H_2O, 0.25 M Glc, 25.0 mM $AlCl_3$ or not, subtraction of reference water spectrum at 298 K. (ν = 1055 cm^{-1}, α-D-Glc; ν = 1080 cm^{-1}, β-D-Glc; ν = 1156 cm^{-1}, deforming of pyranoid ring).

(α-D-Glc) decreased and that of 1080 cm^{-1} (β-D-Glc)[47−49] increased, indicating the occurrence of a mutarotation process. The intensity of the band at 1156 cm^{-1} decreased with time, revealing that the mutarotation process led to the ring-opening of glucose. With the addition of $AlCl_3$, less time was required to reach the anomeric equilibration (90 min vs 120 min). That is, the ring-opening process was accelerated by the presence of $[Al(OH)_2(aq)]^+$ species. However, the direct evidence for the role of OH in active $[Al(OH)_2(aq)]^+$ species on the ring-opening process of glucose was hardly to be observed under the present conditions because of the very fast proton exchange between solute and solvent water.[51]

Mechanism of Glucose-to-Fructose Isomerization. After the ring-opening of cyclic glucose, the interaction between $[Al(OH)_2(aq)]^+$ species and acyclic glucose in the reaction process was investigated by introducing additives (glycerol (GLY), glyceraldehyde (GLA), or 1,3-dihydroxyacetone (DHA)) whose structures were similar to that of acyclic glucose. The competitive interaction with active aluminum species between glucose and additive molecules will influence the isomerization of glucose to fructose. The results are shown in Table 2.

Table 2. Influence of Additives on Glucose-to-Fructose Isomerization[a]

entry	additive	X (%)	Y_{Fru} (%)
1	none	31.8	26.3
2[b]	GLY	33.7	25.1
3[b]	GLA	21.4	9.1
4[b]	DHA	21.9	7.2

[a]Reaction conditions: 1.0 mL H_2O, 0.25 M Glc, 25.0 mM $AlCl_3$, 393 K, 180 min. [b]0.125 M Glc, 0.125 M additives.

From the Fischer projection perspective, acyclic glucose could be considered as one GLY molecule attached to one GLA molecule, while DHA has similar structural feature as GLA that contains carbonyl group in structure (Figure S9).[40] When GLA was added into the aqueous glucose solution, both the conversion of glucose and the yield of fructose were lowered, indicating the possible interaction between active aluminum species and GLA which slowed down the rate of glucose-to-fructose isomerization. DHA exhibited similar influence on the isomerization of glucose, while GLY had no such influence because of the shortage of carbonyl group in its structure. The results indicated that the active $[Al(OH)_2(aq)]^+$ species tended to interact with carbonyl group on acyclic glucose, which might lead to the hydride shift in the aldose-to-ketose isomerization. These results also support the ring-opening mechanism for the isomerization process.

When C2 D-labeled glucose was used as the reactant, the remaining sugar fractions were separated from the mixture by lyophilization after the $AlCl_3$-catalyzed reaction. The ^{13}C and ^1H NMR spectra showed that the structure of unreacted C2 D-labeled glucose remained unchanged, while those of the produced fructose were different to the standard spectra of unlabeled fructose (Figure S10, S11).[40] The appearance of the very low-intensity triplets at δ = 66.6 and 65.4 ppm in the ^{13}C NMR signal of the produced fructose suggested the deuterium shift from C2 position of C2 D-labeled glucose to C1 position of produced fructose (Figure S10).[40] Besides, as revealed in Figure S11,[40] the resonance peak at δ = 3.46 ppm in the ^1H NMR of unlabeled fructose was not observed in that of produced fructose, owing to the replacement of one hydrogen atom with one deuterium atom. These results clearly supported an intramolecular hydride shift mechanism catalyzed by $AlCl_3$.[6,18] These results also indirectly explained that the

DOI: 10.1021/acscatal.5b01237
ACS Catal. 2015, 5, 5097−5103

Scheme 2. Mechanism of Glucose-to-Fructose Isomerization in Water Catalyzed by $AlCl_3$

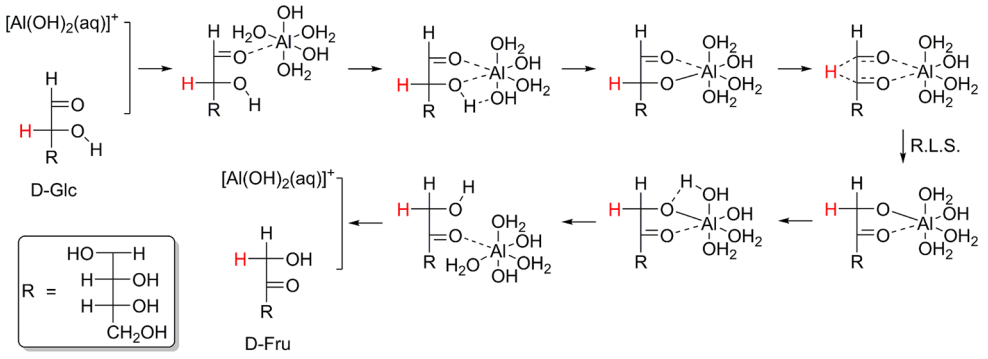

coordination of Al with acyclic glucose on the C1−O and C2−O positions facilitated the following intramolecular C2 → C1 hydride shift.

Obvious kinetic isotopic effects (KIEs) were observed when C2 D-labeled glucose was used as the reactant. This result proved that the hydride shift from C2 to C1 positions of glucose was the rate-limiting step.[6,18] As shown in Table S3,[40] it seemed that the concentration of $AlCl_3$ had no obvious influence on the KIE value (k_H/k_D = 2.7 ± 0.3). The higher KIE value when compared with that discovered by Choudhary[18] (1.71 ± 0.10) was possibly due to the difference in reaction conditions applied. On the basis of these results, a detailed mechanism of glucose-to-fructose isomerization in water catalyzed by $AlCl_3$ is illustrated in Scheme 2.

CONCLUSIONS

In summary, a detailed mechanism of $AlCl_3$-catalyzed glucose-to-fructose isomerization in aqueous media was proposed. As a cheap and low-toxic Lewis acid catalyst, $AlCl_3$ behaved well in the glucose-to-fructose isomerization in water with high fructose selectivity and good carbon balance. The E_a was estimated to be 110 ± 2 kJ·mol^{-1} over 373−403 K. The $[Al(OH)_2(aq)]^+$ species contributed a lot to the isomerization reaction. The $[Al(OH)_2(aq)]^+$ species accelerated the ring-opening of glucose and coordinated with acyclic glucose on the C1−O and C2−O positions to initiate the intramolecular hydride shift. The aluminum center kept its hexa-coordination throughout the isomerization reaction.

ASSOCIATED CONTENT

Supporting Information

The Supporting Information is available free of charge on the ACS Publications website at DOI: 10.1021/acscatal.5b01237.

Further details of kinetics data, activity comparisons of different catalysts, ESI-MS spectra, $^1H/^{13}C/^{27}Al$ NMR spectra, and the results of some control experiments (PDF)

AUTHOR INFORMATION

Corresponding Authors

*E-mail: changweihu@scu.edu.cn (C.H.).

*E-mail: zhulf@scu.edu.cn (L.Z.). Tel./Fax: (+86) 028-85411105.

Notes

The authors declare no competing financial interest.

ACKNOWLEDGMENTS

This work was financially supported by the National Basic Research Program of China (973 program, No. 2013CB228103) and the Special Research Fund for the Doctoral Program of Higher Education (No. 20120181130014) of China. The characterization from the Analytical and Testing Center of Sichuan University was greatly appreciated.

REFERENCES

(1) van Putten, R. J.; van der Waal, J. C.; de Jong, E.; Rasrendra, C. B.; Heeres, H. J.; de Vries, J. G. *Chem. Rev.* **2013**, *113*, 1499−1597.
(2) Nakagawa, Y.; Tamura, M.; Tomishige, K. *ACS Catal.* **2013**, *3*, 2655−2668.
(3) Saha, B.; Abu-Omar, M. M. *Green Chem.* **2014**, *16*, 24−38.
(4) Teong, S. P.; Yi, G.; Zhang, Y. *Green Chem.* **2014**, *16*, 2015−2026.
(5) Moliner, M.; Román-Leshkov, Y.; Davis, M. E. *Proc. Natl. Acad. Sci. U. S. A.* **2010**, *107*, 6164−6168.
(6) Román-Leshkov, Y.; Moliner, M.; Labinger, J. A.; Davis, M. E. *Angew. Chem., Int. Ed.* **2010**, *49*, 8954−8957.
(7) Bermejo-Deval, R.; Gounder, R.; Davis, M. E. *ACS Catal.* **2012**, *2*, 2705−2713.
(8) Bermejo-Deval, R.; Orazov, M.; Gounder, R.; Hwang, S.-J.; Davis, M. E. *ACS Catal.* **2014**, *4*, 2288−2297.
(9) Rajabbeigi, N.; Torres, A. I.; Lew, C. M.; Elyassi, B.; Ren, L.; Wang, Z.; Je Cho, H.; Fan, W.; Daoutidis, P.; Tsapatsis, M. *Chem. Eng. Sci.* **2014**, *116*, 235−242.
(10) Bermejo-Deval, R.; Assary, R. S.; Nikolla, E.; Moliner, M.; Roman-Leshkov, Y.; Hwang, S. J.; Palsdottir, A.; Silverman, D.; Lobo, R. F.; Curtiss, L. A.; Davis, M. E. *Proc. Natl. Acad. Sci. U. S. A.* **2012**, *109*, 9727−9732.
(11) Saravanamurugan, S.; Paniagua, M.; Melero, J. A.; Riisager, A. *J. Am. Chem. Soc.* **2013**, *135*, 5246−5249.
(12) Souza, R. O. L.; Fabiano, D. P.; Feche, C.; Rataboul, F.; Cardoso, D.; Essayem, N. *Catal. Today* **2012**, *195*, 114−119.
(13) Akiyama, G.; Matsuda, R.; Sato, H.; Kitagawa, S. *Chem. - Asian J.* **2014**, *9*, 2772−2777.
(14) Son, P. A.; Nishimura, S.; Ebitani, K. *React. Kinet., Mech. Catal.* **2014**, *111*, 183−197.
(15) Delidovich, I.; Palkovits, R. *Catal. Sci. Technol.* **2014**, *4*, 4322−4329.
(16) Delidovich, I.; Palkovits, R. *J. Catal.* **2015**, *327*, 1−9.
(17) Choudhary, V.; Mushrif, S. H.; Ho, C.; Anderko, A.; Nikolakis, V.; Marinkovic, N. S.; Frenkel, A. I.; Sandler, S. I.; Vlachos, D. G. *J. Am. Chem. Soc.* **2013**, *135*, 3997−4006.
(18) Choudhary, V.; Pinar, A. B.; Lobo, R. F.; Vlachos, D. G.; Sandler, S. I. *ChemSusChem* **2013**, *6*, 2369−2376.
(19) Mushrif, S. H.; Varghese, J. J.; Vlachos, D. G. *Phys. Chem. Chem. Phys.* **2014**, *16*, 19564−19572.
(20) Jia, S.; Liu, K.; Xu, Z.; Yan, P.; Xu, W.; Liu, X.; Zhang, Z. C. *Catal. Today* **2014**, *234*, 83−90.

DOI: 10.1021/acscatal.5b01237
ACS Catal. 2015, 5, 5097−5103

(21) Enslow, K. R.; Bell, A. T. *Catal. Sci. Technol.* **2015**, *5*, 2839−2847.
(22) De, S.; Dutta, S.; Saha, B. *Green Chem.* **2011**, *13*, 2859−2868.
(23) Yang, Y.; Hu, C.; Abu-Omar, M. M. *J. Mol. Catal. A: Chem.* **2013**, *376*, 98−102.
(24) Pagán-Torres, Y. J.; Wang, T.; Gallo, J. M. R.; Shanks, B. H.; Dumesic, J. A. *ACS Catal.* **2012**, *2*, 930−934.
(25) Rasrendra, C. B.; Makertihartha, I. G. B. N.; Adisasmito, S.; Heeres, H. J. *Top. Catal.* **2010**, *53*, 1241−1247.
(26) Yang, Y.; Hu, C.-w.; Abu-Omar, M. M. *Green Chem.* **2012**, *14*, 509−513.
(27) Zhang, X.; Hewetson, B. B.; Mosier, N. S. *Energy Fuels* **2015**, *29*, 2387−2393.
(28) Liu, C.; Carraher, J. M.; Swedberg, J. L.; Herndon, C. R.; Fleitman, C. N.; Tessonnier, J.-P. *ACS Catal.* **2014**, *4*, 4295−4298.
(29) Carraher, J. M.; Fleitman, C. N.; Tessonnier, J.-P. *ACS Catal.* **2015**, *5*, 3162−3173.
(30) Qian, X. *Top. Catal.* **2012**, *55*, 218−226.
(31) Silva, A. M.; da Silva, E. C.; da Silva, C. O. *Carbohydr. Res.* **2006**, *341*, 1029−1040.
(32) Qian, X. *J. Phys. Chem. B* **2013**, *117*, 11460−11465.
(33) Caratzoulas, S.; Davis, M. E.; Gorte, R. J.; Gounder, R.; Lobo, R. F.; Nikolakis, V.; Sandler, S. I.; Snyder, M. A.; Tsapatsis, M.; Vlachos, D. G. *J. Phys. Chem. C* **2014**, *118*, 22815−22833.
(34) Tzoupanos, N. D.; Zouboulis, A. I.; Tsoleridis, C. A. *Colloids Surf., A* **2009**, *342*, 30−39.
(35) Swaddle, T. W.; Rosenqvist, J.; Yu, P.; Bylaska, E.; Phillips, B. L.; Casey, W. H. *Science* **2005**, *308*, 1450−1453.
(36) Urabe, T.; Tanaka, M.; Kumakura, S.; Tsugoshi, T. *J. Mass Spectrom.* **2007**, *42*, 591−597.
(37) Urabe, T.; Tsugoshi, T.; Tanaka, M. *J. Mol. Liq.* **2008**, *143*, 70−74.
(38) Shafran, K.; Deschaume, O.; Perry, C. C. *Adv. Eng. Mater.* **2004**, *6*, 836−839.
(39) He, M.; Fu, H.; Su, B.; Yang, H.; Tang, J.; Hu, C. *J. Phys. Chem. B* **2014**, *118*, 13890−13902.
(40) See the Supporting Information for details.
(41) Lecomte, J.; Finiels, A.; Moreau, C. *Starch/Stärke* **2002**, *54*, 75−79.
(42) Asaoka, H. *Carbohydr. Res.* **1985**, *137*, 99−109.
(43) Kooyman, C.; Vellenga, K.; De Wilt, H. G. J. *Carbohydr. Res.* **1977**, *54*, 33−44.
(44) Akitt, J. W. *Prog. Nucl. Magn. Reson. Spectrosc.* **1989**, *21*, 1−149.
(45) Akitt, J. W.; Mann, B. E. *J. Magn. Reson.* **1981**, *44*, 584−589.
(46) Öhman, L.-O.; Edlund, U. Aluminum-27 NMR of Solutions. In *Encyclopedia of Nuclear Magnetic Resonance*; Grant, D. M., Harris, R. K., Eds.; John Wiley & Sons: Chichester, UK, 1996; Vol. *2*, pp 742−751.
(47) Back, D. M.; Michalska, D. F.; Polavarapu, P. L. *Appl. Spectrosc.* **1984**, *38*, 173−180.
(48) Back, D. M.; Polavarapu, P. L. *Carbohydr. Res.* **1983**, *121*, 308−311.
(49) Kanou, M.; Nakanishi, K.; Hashimoto, A.; Kameoka, T. *Appl. Spectrosc.* **2005**, *59*, 885−892.
(50) Bubb, W. A. *Concepts Magn. Reson.* **2003**, *19A*, 1−19.
(51) Faust, B. C.; Labiosa, W. B.; Dai, K. o. H.; MacFall, J. S.; Browne, B. A.; Ribeiro, A. A.; Richter, D. D. *Geochim. Cosmochim. Acta* **1995**, *59*, 2651−2661.

DOI: 10.1021/acscatal.5b01237
ACS Catal. 2015, 5, 5097−5103